ORIGINAL

Matti-P. Sarén · Ritva Serimaa

Determination of microfibril angle distribution by X-ray diffraction

Abstract X-ray diffraction is a well-established method for the determination of the mean microfibril angle (MFA). When the sample is a slice of wood variations in the fibre orientation, the shape of the cells, and the measurement geometry affect the intensity curve. A general form for diffraction conditions in terms of angles describing the fibre orientation and the shape of the cell was derived. Intensity curves were calculated by using Monte Carlo method and compared with experimental ones. Both peak fitting and variance methods were used for determining the mean MFA from the intensity curves. Norway spruce was used as an example. Results indicate that deviations in the fibre orientation, the spiral grain, do not affect the mean MFA considerably when using the symmetrical transmission geometry. When using the perpendicular transmission geometry large deviations in spiral grain or tips tend to increase the MFA determined with the variance method and decrease the MFA determined with the fitting method. The shape of the cell should be considered when using the reflection 200 and the fitting method. The variance method is insensitive to the shape of the cell.

Abbreviations

MFA	Microfibril angle
XRD	X-ray diffraction
PTG	Perpendicular transmission geometry
STG	Symmetrical transmission geometry
STD	Standard deviation

Matti-P. Sarén (✉)
Measurement and Sensor Laboratory, University of Oulu, Teknologiapuisto 127, 87400, Kajaani, Finland
E-mail: matti.saren@oulu.fi

R. Serimaa · Matti-P. Sarén
Division of X-ray Physics, Department of Physical Sciences, University of Helsinki, P.O. Box 64, 00014, Helsinki, Finland

Introduction

Cell walls of softwood tracheids consist of thin primary cell wall and thick secondary cell wall, which is composed of several layers. The main constituent of the cell wall is cellulose, which forms long, partly crystalline, and helically wound microfibrils. In Norway spruce, the diameter of crystallites is about 3.1 nm and the length is about 30 nm (Andersson et al. 2003). The angle between the microfibril and the cell axis is called the microfibril angle (MFA). The orientation of microfibrils in the thick S_2 layer of the secondary cell wall has been argued to be a principal predictor of wood quality, with density behaving as an auxiliary variable (Cave and Walker 1994). The longitudinal shrinkage was reported to decrease with diminishing MFA (Harris and Meylan 1965). MFA has been shown to play an important role in keeping the developing stem mechanically stable in changing environmental conditions (Booker and Sell 1998; Lichtenegger et al. 1999).

X-ray diffraction (XRD) is a well-established method for determining MFA (e.g. Cave 1966; 1997a, b). Many other methods, such as polarized light (Donaldson 1991; Ye et al. 1994), confocal (Batchelor et al. 1997; Verbelen and Stickens 1995), and electron microscopy (Abe et al. 1991), and soft-rot induced cavities (Bailey and Vestal 1937; Anagnoste et al. 2000) are also used. Most of these methods, however, are destructive, tedious, and time consuming and thus not applicable for large sets of samples.

Regardless of the measurement geometry and the preparation of the sample, data analysis of XRD measurements is complicated. Determination of MFA is a special case of a texture measurement, simplified by the assumption of the fibre symmetry and the structure of wood cells. Cave (1966) presented diffraction conditions for cellulose crystallites for the perpendicular transmission geometry (PTG). In that paper intensity profiles of the 200 reflection were calculated for cells with round and square cross sections and the effect of misalignment of the sample was considered. Here, reflections are indexed according to Nishiyama et al. (2002), in which the unit cell is monoclinic, $P2_1$, with $a = 0.7784(8)$ nm, $b = 0.8201(8)$ nm, $c = 1.0380(10)$ nm and $\gamma = 96.5°$. In Cave (1966), the MFA distribution was assumed Gaussian and the T-parameter method was introduced for determining MFA. T-parameter is affected by the cross-sectional shape of the cells (Cave 1966) and Yamamoto (1993) attempted to refine this method by improving the calculation of the mean MFA from the T-parameter. In order to eliminate the effect of the shape of the cross section of the cell, Evans (1999) presented a method based on a variance approach for determining MFA. Prud'homme and Noah (1975) proposed a method for determining the MFA distribution by using the 200 reflection for cells with a circular cross section.

Peura et al. (2005) determined the MFA distribution in a single cell wall using a very small X-ray beam guided through a bordered pit and showed that the shape of the MFA distribution usually differs from Gaussian for Norway spruce. Furthermore, the local mean orientation of the cellulose microfibrils in the cell wall was studied using a small synchrotron beam and PTG and samples cut perpendicularly to longitudinal axis of the cell (Lichtenegger et al. 1999; Paris and Müller 2003), but variations in the MFA in different cell wall layers were not quantified.

Lotfy et al. (1973) used the symmetrical transmission geometry (STG) and considered the reflection 004. They developed a numerical method for determining MFA, which is applicable also for other reflections and different cross-sectional shapes of the cells. The intensity curve of the reflection 004 is unaffected by the shape of the cross section of the cells. Unfortunately, there are other reflections close to it complicating the data analysis (Lofty et al. 1973; Andersson et al. 2000). Paakkari and Serimaa (1984) presented data analysis based on curve fitting and considered the separation of the contributions of S_1, S_2 and S_3 layers from the measured intensity curve. Cave (1997a, b) examined analysis of the reflections 200 and 004 together in order to find the average MFA distribution. By that means it is possible to determine both the average shape of the cross section of the cells and MFA (Andersson et al. 2000).

Wood cells are not perfectly parallel to each other in a wood sample as one usually assumes in order to simplify the determination of MFA. The deviation of the direction of tracheids from the longitudinal direction in a tree is called the spiral grain, and it can be found in practically every tree (Kozlowski and Winget 1963). The spiral grain may change between early and latewood (Wobst et al. 1994; Sarén et al. 2005b). Therefore, in this work, we investigate the effects of variations in the fibre and cell wall orientation on the obtained MFA and use Norway spruce as an example. Variation in the cross-sectional shape was studied with optical microscopy. For the calculations, we combine findings of several papers to a single mathematical treatment. With the aid of it, properties of X-ray set-ups with STG or PTG and their data analysis are discussed.

Theory

According to the elementary diffraction theory the diffraction conditions are met when

$$\frac{s_{diff} - s_{in}}{\lambda} = s = r^*_{hkl}, \text{ and } |s| = \frac{2 \sin \theta}{\lambda} = \frac{1}{d_{hkl}} \tag{1}$$

where s is the scattering vector, s_{diff} and s_{in} are the wave vectors of the diffracted and incident X-ray beams, respectively, 2θ is the scattering angle, λ is the wavelength, r_{hkl}^* is the reciprocal lattice vector, and d_{hkl} is the lattice spacing. (e.g. Guinier 1994)

The scattering angle for the cellulose reflection 004 is ca. $34.2°$ (Nishiyama et al. 2002), when CuKα radiation is used. The normal of the (004) planes is parallel to the cellulose chains. For CuKα radiation the scattering angle for the strong reflection 200 is about $22.8°$. The (200) planes are parallel to the cellulose chains. Because a- and b-axes are uniformly distributed about the cell axis (Lichtenegger et al. 1999), the reciprocal lattice vectors that are not parallel to the reciprocal lattice vector of the plane (004) form a cone around this direction. Due to this symmetry, the diffraction conditions can be written

$$\frac{s \cdot r^*_{hkl}}{|s| \cdot |r^*_{hkl}|} = \cos \alpha, \tag{2}$$

where α is the space angle between the reciprocal lattice vector of (004) plane and the reciprocal lattice vector of the plane investigated. Therefore, $\alpha = 0°$ and

$\alpha = 90°$ for the reflections 004 and 002, respectively. The aim of the following calculation is to obtain the intensity curve, $I(\phi)$, of the reflection *hkl* as a function of ϕ, which is the azimuth angle in the detector plane (Fig. 1).

Scattering vector

In PTG the detector plane is perpendicular to the incident beam (Fig. 1). The angle between the incident and diffracted beam is 2θ and ϕ is the azimuth angle in the detector plane (Fig. 1). In laboratory co-ordinates ($\mathbf{e}_1$, $\mathbf{e}_2$ and $\mathbf{e}_3$) the incident beam hits the sample at origin from the negative direction of $\mathbf{e}_2$. The direction of the scattering vector $\mathbf{s}$ is given by the angles δ and ϕ. The angle δ is the angle between the scattering vector and $\mathbf{e}_1$, $\mathbf{e}_3$-plane, counter clockwise from the positive axis of $\mathbf{e}_1$, and in the case of PTG $\delta = 0$. The unit vector parallel to the scattering vector $\mathbf{s}$ is given in laboratory co-ordinates by

$$\widehat{\mathbf{s}} = \begin{bmatrix} \cos\phi & 0 & \sin\phi \\ 0 & 1 & 0 \\ -\sin\phi & 0 & \cos\phi \end{bmatrix} \begin{bmatrix} 0 \\ -\sin\delta \\ \cos\delta \end{bmatrix} = \begin{bmatrix} \sin\phi\cos\delta \\ -\sin\delta \\ \cos\phi\cos\delta \end{bmatrix} \tag{3}$$

For PTG the scattering vectors for each reflection form a cone, with an apex in the origin and an opening angle of $180° - 2\theta$.

When STG is used, both the incident and diffracted beam are in $\mathbf{e}_2$, $\mathbf{e}_3$ -plane (Fig. 2), and the angle between the incident beam and $\mathbf{e}_2$ -axis and the angle between the diffracted beam and the axis $\mathbf{e}_2$ is θ. Thus the scattering vector is parallel to $\mathbf{e}_3$-axis ($\delta = 0°$). The sample is rotated around its normal ($\mathbf{e}_2$-axis) and the diffracted intensity is measured as a function of the rotation angle. However, from the point of view of the diffraction condition rotation of the sample around its normal and solving diffraction conditions as a function of ϕ are analogous. Thus, both STG and PTG can be treated together.
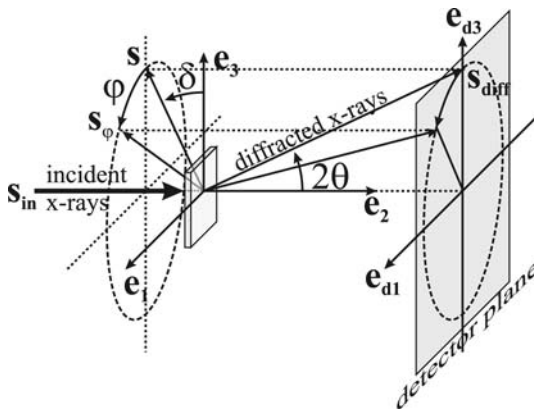
Fig. 1 Perpendicular transmission geometry (PTG). The incident beam and the detector are perpendicular to the surface of the sample. The diffraction pattern is recorded with a position sensitive detector. Incident beam is parallel to $\mathbf{e}_2$ and the angle between the incident and diffracted beam is 2θ
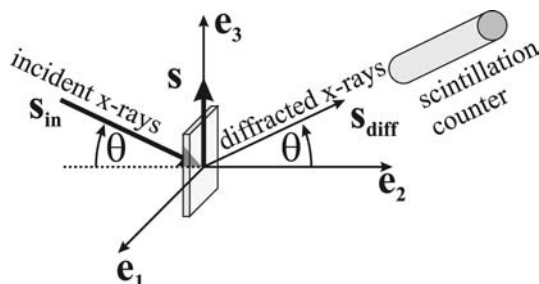
Fig. 2 Symmetrical transmission geometry (STG). The X-ray beam and the scintillation counter are at the angle θ with respect to the normal of the surface of the sample. The sample is rotated about the normal of its surface and the intensity is measured as a function of the rotation angle

Reciprocal lattice vectors

Let one assume that the longitudinal direction of the sample is parallel to the axis $\mathbf{e}_3$ and that the surface of the sample is perpendicular to the axis $\mathbf{e}_2$. The reciprocal lattice vector $\mathbf{r}_{00l}^*$ is parallel to the direction of the microfibril and the c-axis of cellulose unit cell. The angle μ is the MFA, which is the angle between $\mathbf{r}_{00l}^*$ and the positive $\mathbf{e}_3$-axis (Fig. 3a). The angle γ is the azimuth angle of the normal of the cell wall seen in counter clockwise direction from the positive $\mathbf{e}_3$-axis. The unit vector $\hat{\mathbf{r}}_{00l}^*$ is given by

$$\hat{\mathbf{r}}_{00l}^* = \begin{bmatrix} \sin \mu \cos \gamma \\ \sin \mu \sin \gamma \\ \cos \mu \end{bmatrix} \tag{4}$$

To calculate the intensity profile for samples where not all fibres are parallel, (e.g. spiral-graining) angles ρ and ω are introduced. The angle ρ is the angle between the axis $\mathbf{e}_1$ and the longitudinal direction of a cell, in counter clockwise direction seen from positive axis (Fig. 3b). The angle ω is the angle between the axis $\mathbf{e}_2$ and the longitudinal direction of a cell, in counter clockwise direction seen from positive axis (Fig. 3c). The vector $\hat{\mathbf{r}}_{00l}^*$ is now given by
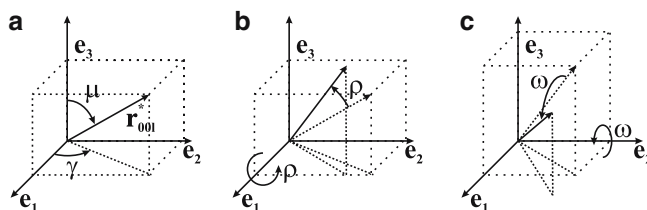
Fig. 3 The direction of the cellulose chains. This is the same as the direction of the reciprocal lattice vector $\mathbf{r}_{001}^*$ of the (004) plane (**a**). The angle μ is the microfibril angle and γ is the azimuth angle of the cell wall. To take into account the fact that not all cells are parallel to the longitudinal direction ($\mathbf{e}_3$), $\mathbf{r}_{001}^*$ is first rotated by the angle ρ around $\mathbf{e}_1$ (**b**) and then around $\mathbf{e}_2$ by the angle ω (**c**)

$$\hat{\mathbf{r}}_{00l}^* = \begin{bmatrix} \cos\omega & 0 & \sin\omega \\ 0 & 1 & 0 \\ -\sin\omega & 0 & \cos\omega \end{bmatrix} \cdot \begin{bmatrix} 1 & 0 & 0 \\ 0 & \cos\rho & -\sin\rho \\ 0 & \sin\rho & \cos\rho \end{bmatrix} \cdot \begin{bmatrix} \sin\mu\cos\gamma \\ \sin\mu\sin\gamma \\ \cos\mu \end{bmatrix}$$
$$= \begin{bmatrix} \cos\gamma\cos\omega\sin\mu + \sin\omega(\cos\mu\cos\rho + \sin\gamma\sin\mu\sin\rho) \\ \cos\rho\sin\gamma\sin\mu - \cos\mu\sin\rho \\ \cos\omega(\cos\mu\cos\rho + \sin\gamma\sin\mu\sin\rho) - \cos\gamma\sin\mu\sin\omega \end{bmatrix} \tag{5}$$

Diffraction conditions

Combining Eqs. 2, 3, and 5 the diffraction condition is given by

$$\hat{\mathbf{s}} \cdot \pm\hat{\mathbf{r}}_{00l}^* = \pm(\sin(\phi-\omega)\cos\delta\sin\mu\cos\gamma - \sin\delta(\cos\rho\sin\mu\sin\gamma - \sin\rho\cos\mu) \\ + \cos\delta\cos(\phi-\omega)(\sin\rho\sin\mu\sin\gamma + \cos\rho\cos\mu)) = \cos\alpha. \tag{6}$$

The plus minus sign is added to the reciprocal lattice vector in order to take into account its possible orientations during rotations. The behaviour of the azimuth angle ϕ is needed as a function of μ for data analysis. It can be solved from Eq. 6 by manipulating it to the form

$$A\cos\vartheta + B\sin\vartheta = \Psi\cos(\vartheta - \Phi) = C, \tag{7}$$

where the amplitude $\Psi = \sqrt{A^2 + B^2}$, the phase $\Phi = \arctan(B/A) + m\pi$, where $m = 1$ if $A > 0$ and else $m = 0$. Thus position of the intensity maximum as a function of $\phi-\omega$ resulting from cellulose crystallites that are oriented to the single direction (μ, γ) as a function of angles ρ, δ, ω, and α calculated from Eq. 6 is

$$\phi - \omega = \arctan\left(\tfrac{B}{A}\right) \pm \arccos\left(\tfrac{C}{\sqrt{A^2+B^2}}\right) + m\pi, \text{ where}$$
$$A = \cos\delta\sin\rho\sin\mu\sin\gamma + \cos\delta\cos\rho\cos\mu$$
$$B = \cos\delta\sin\mu\cos\gamma \tag{8}$$
$$C = \pm\cos\alpha + \sin\delta\cos\rho\sin\mu\sin\gamma - \sin\delta\sin\rho\cos\mu.$$

MFA is here considered as a random variable and intensity depends on its probability density. An analytical expression can be derived considering transformations of probability densities for the diffracted intensity (Cave 1997a, b). However, the formulas obtained from Eq. 8 would become too complicated for practical work. In this paper, the diffracted intensity is calculated using the Monte Carlo method.

Perpendicular transmission geometry

In the PTG the angle between the scattering vector and the surface of the sample is $\delta = \theta$, where 2θ is the scattering angle (Fig. 1). The sample is assumed to be perfectly oriented and to have cells with rectangular cross sections. The longitudinal direction of the cells is parallel to the axis $\mathbf{e}_3$, and the angles ρ and ω are 0°. The shape of the cross section of the cell is taken into account in

the angle γ. For cells with rectangular cross sections $\gamma = 0°$, $\pm 90°$, or $180°$. For the cell walls that are perpendicular to the incident beam ($\gamma = 0°$, or $180°$), Eq. 6 simplifies

$$\cos\mu\cos\varphi \pm \sin\mu\sin\varphi = \pm\cos\alpha/\cos\theta. \tag{9}$$

It is straightforward to verify that solutions for the reflection 200 are $\phi = \mu \pm 90°$, for $\gamma = 0°$ and $\phi = -\mu \pm 90°$ for $\gamma = 180°$. For other cell walls $\gamma = \pm 90°$

$$\cos\phi = \frac{\pm\sin\mu\sin\theta \pm \cos\alpha}{\cos\mu\cos\theta}. \tag{10}$$

This equation is analogous to Eq. 10-3 presented in Klug and Alexander (1974). For the reflection 200 solutions are more complicated; the diffracted intensity is concentrated near the angles $\phi = \pm 90°$.

For the reflection 004 the only solution of Eq. 10 is $\mu = \theta$, when $\gamma = -90°$ and $\mu = -\theta$, when $\gamma = 90°$. For Eq. 9, there are no solutions for the 004 reflection, because $-1 < \cos\mu\cos\phi \pm \sin\mu\sin\phi < 1$ and $\cos\alpha/\cos\theta > 1$. Therefore, for an ideal cell the diffracted intensity has no dependence on MFA.

Lichtenegger et al. (1999) suggested a novel diffraction experiment for determination of MFA. In this set-up, a thin cross section of wood is placed perpendicularly to a very narrow incident beam in such way that the longitudinal direction of the cells is parallel to the incident beam. This method is interesting since it may allow one to determine the MFA for S_3 and S_1 layers. For this geometry parameters of Eq. 6 are $\gamma = \omega = 0°$ and $\alpha = \rho = 90°$ (Paris and Müller 2003).

Symmetrical transmission geometry

In STG the scattering vector is parallel to the surface of the sample (Fig. 2) and $\delta = 0°$. The longitudinal direction of the cells is assumed to be parallel to the axis e_3, therefore angles ρ and ω are $0°$. Equation 6 simplifies now to

$$\cos\mu\cos\phi + \sin\mu\sin\phi\cos\gamma = \cos\alpha. \tag{11}$$

Let the cross sections of the cells be rectangular. It is straightforward to verify that the solutions for the reflection 200 are the same as for PTG; $\phi = \mu \pm 90°$, for $\gamma = 0°$ and $\phi = \mu \pm 90°$ for $\gamma = 180°$. For cell walls $\gamma = 90°$ and $\gamma = -90°$ solutions are $\phi = -90°$ and $\phi = -90°$, respectively.

For the 004 reflection the solutions for the cell walls $\gamma = 0°$ and $\gamma = 180°$ are $\phi = \mu$ and $\phi = -\mu$, respectively. For all other cell walls, there is only one solution, $\mu = 0°$. This means that the intensity as a function of ϕ is independent of the shape of the cross section of the cells.

When the cross section of the cells is round, one should note that the shape of the intensity curve is the same for STG and PTG, when the 200 reflection is used. The diffraction condition for the 004 reflection is met when cellulose chains are parallel to the scattering vector. This is the case for STG, when cellulose chains are running in e_1, e_3-plane. In PTG no single direction of cellulose chains can be linked directly to the diffracted intensity.

Experimental

Variations in the cell wall orientation were estimated experimentally using microscopy, XRD and laser light scattering (Sarén et al. 2005a, b) and their effects on the diffracted intensity were studied. Norway spruce (Picea abies [L] Karst.) samples from Ruotsinkylä (lat. 60.21 N, long. 24.59 E), Finland, were used. The same samples were used also in previous papers (Sarén et al. 2001, 2004). The clear wood samples were prepared from stem 1 at the second and 20th and from stem 2 at the fifth and 20th annual ring at breast height (1.3 m). One compression wood sample was also prepared at the 25th annual ring from stem 3.

For X-ray measurements with STG samples of radial thickness of 1 mm were cut along the tangential direction from one earlywood zone. Measurements were performed with $CuK_{\alpha 1}$ radiation, by rotating the sample, and measuring the intensity using a scintillation detector (Andersson et al. 2000; Sarén et al. 2001).

For PTG cylindrical samples of 1 mm diameter and 10 mm in longitudinal direction of wood were prepared. These samples were measured with Bruker AXS D8 discover-set-up (Bruker AXS, Karlsruhe, Germany). A sample was attached to a holder capable of rotating the sample around its longitudinal axis. The diffraction patterns were recorded using an area detector (Hi-Star).

For microscopy several thin sections 16 μm in thickness and 1 cm^2 in area were made from parallel samples by using cryomicrotome (−16°C). Thin sections were stained with safranine and 20 grey scale images were taken using a digital camera attached to a microscope (Sarén et al. 2001). The resolution of the camera was 1,600×1,200 pixels and the size of the pixel was 0.18 μm. The cell wall was isolated using image processing software (Matlab, The Math-Works, Inc., MA, USA).

Results and discussion

Both the shape of the cells and the orientation of the cells with respect to the surfaces of the sample may affect the MFA determination from a piece of wood using XRD. We first demonstrate these effects with experiments, then estimate the extent of variations of the shape and orientation of the cells in our Norway spruce samples, and finally show their effects on the MFA determined by curve fitting (Paakkari and Serimaa 1984; Sarén et al. 2001, 2004) and the variance approach (Evans 1999) using calculations.

Experimental intensity curves for the reflections 200 and 004 are shown in Fig. 4 for samples with round and rectangular cell cross sections measured with PTG and STG. Fig. 4c, d shows that for cells with round cross sections the intensities for both reflections measured with STG and PTG agree well. This is attributed to the round cells with plenty of crystallites fulfilling the diffraction conditions in both measurement geometries. This sample is from the second annual ring (Sarén et al. 2001) and its mean MFA is 22.2°. Using the variance method (Evans 1999, Eq. 35) MFA of 25.7° is obtained. This might be due to the asymmetry and broadness of the MFA distribution. Furthermore, the calibration of the variance method may not be optimal for these samples.
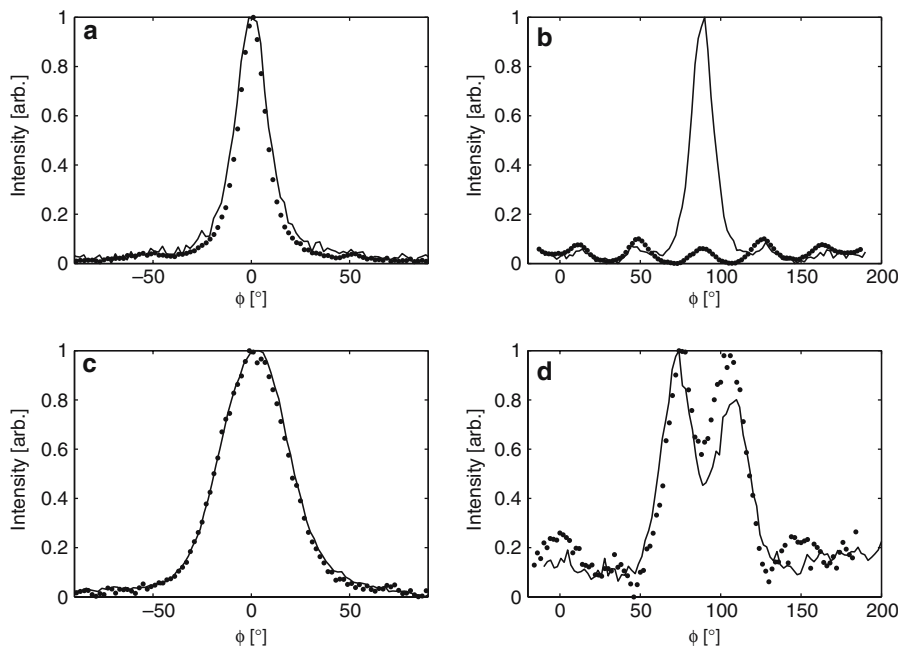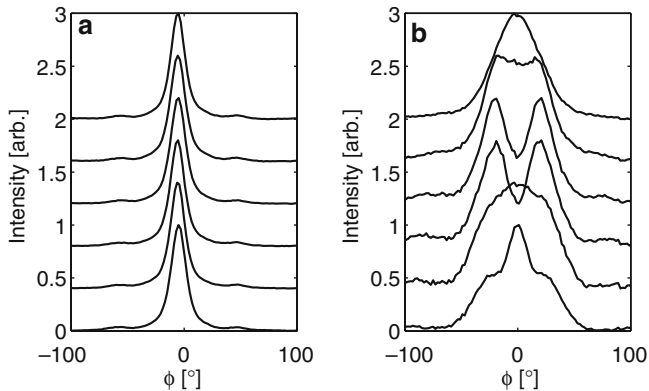
Fig. 4 Intensity profiles for the reflection 200 (**a**, **c**) and 004 (**b**, **d**) for samples from the stem 1, the 20th (**a**, **b**) and 2nd (**c**, **d**) annual rings. *Solid line* and *dots* indicate STG and PTG, respectively

The sample with the rectangular cell cross section is from the 20th annual ring of stem 1 and its mean MFA is small, only 7.0° (Sarén et al. 2001). The intensity profile for the 200 reflection (Fig 4a) is narrower in the case of PTG than STG. In PTG the intensity arising from cell walls with $\gamma = \pm 90°$ is concentrated close to $\phi = 0°$, and therefore the intensity profile is narrower than that obtained with STG. This has been taken into account in fitting by adding an extra peak at $\phi = 0°$. This peak was then omitted when calculating the mean MFA (Sarén et al. 2004). In the variance method, contributions of all cell wall layers are in principle taken into account, and the effect of the extra peak on MFA is only a few degrees. We estimate that for this sample this decrease in MFA would be from 10.2° to 7.1°.

The intensity of the 004 reflection of the sample from the 20th year-ring obtained with PTG is very small compared to that obtained with STG (Fig. 4b, at $60° < \phi < 120°$). This is attributed to the fact that tracheids in this sample are almost parallel to each other. There are very few crystallites with lattice planes (004) fulfilling the diffraction conditions (c.f. Eq. 10, when $\alpha = 0°$). Thus the intensity curve does not give the MFA distribution in cell walls parallel to the surface of the sample. The other peaks in the intensity curve are attributed to reflections near 004 (Andersson et al. 2000).

As another demonstration we determined intensity profiles for the reflection 200 of a cylindrical sample using PTG while rotating the sample around its longitudinal axis. In Fig. 5a, the cell cross sections are rectangular. The rotation of the sample does not change the intensity curve remarkably. This is attributed to the fact that in PTG are always contributions from every cell wall and the mean MFA is small.

Fig. 5 Intensity curves for the reflection 200 of longitudinally cut, cylindrical samples from the stem 1 with a diameter of 1 mm in both radial and tangential direction. In (**a**) the sample is from the 20th and in (**b**) from the 2nd annual ring. The sample is rotated around longitudinal direction with a step of 15°. The lowest curves are obtained when radial direction of the sample is perpendicular to the incident X-ray beam

In Fig. 5b, the cells are round and the intensity curve depends strongly on the orientation of the sample. There are remarkable differences in intensity curves obtained when the radial ($\gamma = 0°$) or tangential ($\gamma = 90°$) cell walls are parallel to the incident beam. This is attributed to the bordered pits in the radial cell walls, which may increase the mean MFA (e.g. Sarén et al. 2004). Furthermore, the preferred orientation of the cell walls, and thereby cellulose crystallites, with respect to tangential and radial directions (Fig. 6a) can be seen when the sample is rotated 45°. There is no clear peak at $\phi = 0°$ at this angle. This is in agreement with experimental data reported by Lichtenegger et al. (2001).

In order to estimate the variation in the cross-sectional shape of the cells thin sections of the samples were investigated with optical microscopy (Sarén et al. 2004). The directions of the cell walls with respect to the tangential direction of the samples were measured and are shown in Fig. 6. These curves represent probability density functions for γ. In the sapwood the cross-sectional shape of the cells is almost rectangular (Sarén et al. 2004). In tangential direction the
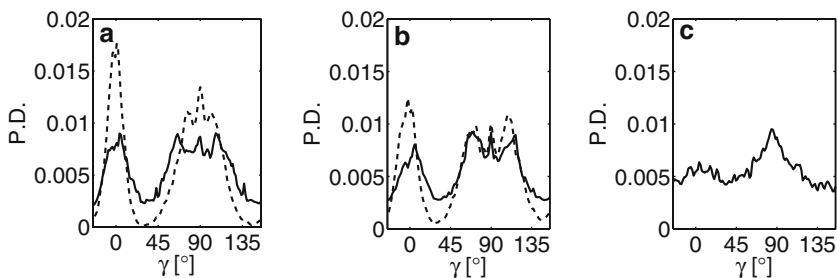

Fig. 6 Probability densities of cell wall orientation as a function of γ. Measurements are made with optical microscopy from the cross sections. The tangential direction is $\gamma = 0°$. In (**a**) (stem 1) and (**b**) (stem 2) *dashed line* indicates a sample from the 20th annual ring and in (**a**) *solid line* indicates a sample from the 2nd and in (**b**) from the 5th annual ring. In (**c**) the probability density for compression wood from the 25th annual ring is shown

orientation of the cell wall is almost Gaussian with standard deviation (STD) 8.7° and 10.3° for stems 1 and 2, respectively. In the radial direction deviations are much larger. Near the pith variations in the cell wall orientation increase and in the compression wood no direction is more pronounced than any other.

The orientation of the cells, like spiral grain and tilted tips of the cells varies in real samples. This cannot be eliminated by sample preparation and may also affect the determined MFA. The spiral grain has been studied thoroughly (e.g. Harris 1988). For Norway spruce, Sarén et al. (2005b) found out that fibres are almost parallel in the radial plane. The variation between the annual rings was less than about 4° whereas in the tangential plane it was up to 15°. Variations in tangential plane within an annual ring were also considerable. These values are estimates for several hundreds of cells.

The following calculations are made for the 200 reflection using Eq. 6 and the Monte Carlo method. The wavelength is equal to $CuK_{\alpha 1}$ radiation. The angles γ, ρ and ω describing the orientation of cells are considered random variables with normal distributions. The variance of γ corresponds to the cross-sectional shape of the cell; if it is small the cross-sectional shape is rectangular. When STD of γ has reached a value of 45° the cross-sectional shape of the cells is practically round. The mean value of γ indicates how well the sample is prepared relative to the radial and tangential directions. The angle γ is zero if the sample is cut parallel to these directions and there are no abnormalities in the sample (e.g. defects during growth). The angle ω represents the cell orientation in the plane parallel to the surface of the sample. The mean value of ρ is linked to the spiral grain and its variance is considered to represent local deviations in spiral grain and tips.

Figure 7 shows calculated intensity curves for a sample having normally distributed MFA with a mean of 15° and STD 5° for STG and PTG. For both geometries the pattern for round cells is almost the same. However, in the case of PTG the intensity maximum around $\phi = \pm 90°$ is more pronounced than in the case of STG. This must be carefully considered when determining the mean
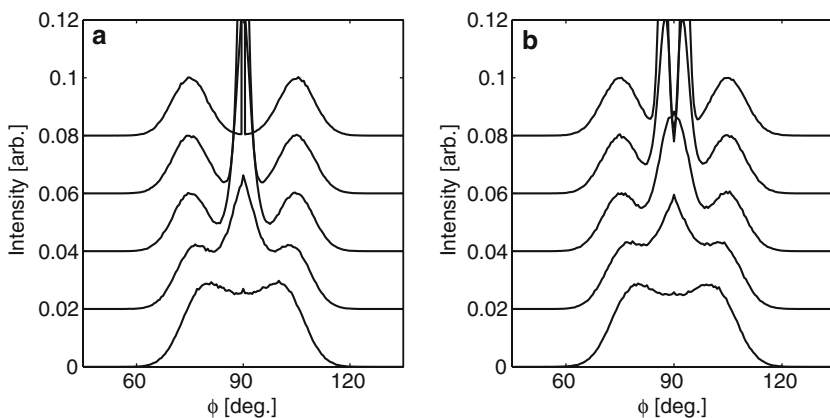
Fig. 7 The effect of cross-sectional shape of the cells. Calculated intensity curves of the reflection 200 as a function of ϕ when the scattering angle $2\theta = 22.8°$ for STG (**a**) and PTG (**b**). Calculations were made for normally distributed MFA with a mean value of 15° and STD of 5°. The standard deviation of γ was 0° (highest curves), 5°, 10°, 20°, or 45° (lowest curves). The values 0° and 45° represent cells with perfect rectangular and round cross sections, respectively

MFA by fitting especially when using PTG. The solved MFA distribution may not be correct if the fitting is not successful.

Table 1 compares the mean MFA values determined from calculated intensity profiles for PTG and STG using the fitting method and for PTG using the variance method (Evans 1999). The STD of MFA obtained by fitting is also given in Table 1. The sample is chosen to be a sapwood sample of Norway spruce. The cells of the sample are assumed to have rectangular cross sections and two cell walls are assumed to be parallel to the surface of the sample. The mean MFA was chosen to be 10° and STD 8°. The MFA is chosen again to be normally distributed. It is assumed that the MFA distribution represents the

Table 1 The mean MFA values determined from calculated intensity profiles for PTG and STG using the fitting method and for PTG using the variance method

$\gamma[°]$		$\rho[°]$		Symmetrical		Perpendicular		Variance method
Mean	STD	Mean	STD	Mean	STD	Mean	STD	μvariance
2	0	0	0	10.0	7.8	10.0	8.4	12.4
5	0	0	0	9.9	7.8	9.6	8.3	12.4
10	0	0	0	9.8	8.0	8.5	8.2	12.4
20	0	0	0	9.4	8.1	6.9	7.8	12.5
45	0	0	0	7.2	7.4	6.3	7.5	12.5
0	2	0	0	10.0	7.9	10.0	8.0	12.4
0	5	0	0	9.8	8.1	9.9	8.3	12.4
0	10	0	0	8.9	8.2	8.9	8.2	12.4
0	20	0	0	7.5	8.6	7.4	8.3	12.6
0	45	0	0	7.0	8.8	6.8	8.6	12.7
0	0	2	0	10.2	8.0	10.0	8.0	12.4
0	0	5	0	10.5	8.0	10.3	8.2	12.4
0	0	10	0	10.5	8.1	10.4	8.3	12.6
0	0	20	0	10.9	8.1	11.2	8.8	13.4
0	0	45	0	14.2	9.2	14.2	9.1	19.5
0	0	0	2	10.0	7.9	10.0	8.0	12.4
0	0	0	5	10.5	8.0	9.6	8.4	12.4
0	0	0	10	10.4	8.1	8.8	8.4	13.0
0	0	0	20	10.8	8.2	8.4	9.7	15.7
0	0	0	45	12.0	9.3	8.1	12.2	31.0

mean MFA distribution of all cells in the sample. This is investigated in the study of Sarén et al. (2005a), where the diffraction patterns of single fibres and pieces of wood are compared. The model, that was fitted to the simulated $I(\phi)$ assumed rectangular cell cross sections and consisted of a pair of Gaussians representing MFA distributions in the front and back wall (Sarén et al. 2001). The results are valid also for larger MFA values. However, then the fitting is easier (Fig. 7).

When the shape of the cell is almost rectangular and there is no spiral grain the fitting method gives the correct mean MFA, 10°, both in the cases of PTG and STG. The variance method gives 12–13° when using Eq. 35, when $\sigma_{add} = 6°$ and $k = 1/3$ (Evans 1999). If the mean value of γ is increased, i.e. the cells are rotated around the axis $\mathbf{e}_3$, the mean MFA determined by fitting decreases. This decrease is larger for PTG than for STG. If the cells cross sections are not rectangular, i.e. the STD of the angle γ increases, the determined mean MFA decreases almost equally for STG and PTG. Figure 8 demonstrates the effect of the shape of the cell in the case of SGT and large MFA. Variations in the angle γ do not change MFA determined with the variance method.

The variations of the orientations of the cells in tangential and radial plane are equal to variations in the angles ρ and ω, respectively for sample cut from one annual ring in tangential direction. The angle ω has a simple relationship with the diffracted intensity (Eq. 6). Its contribution to the intensity curve as a function of ϕ can be presented as a convolution of the intensity profile and the probability density function of angle ω. The deviations in ω widen the intensity curve.
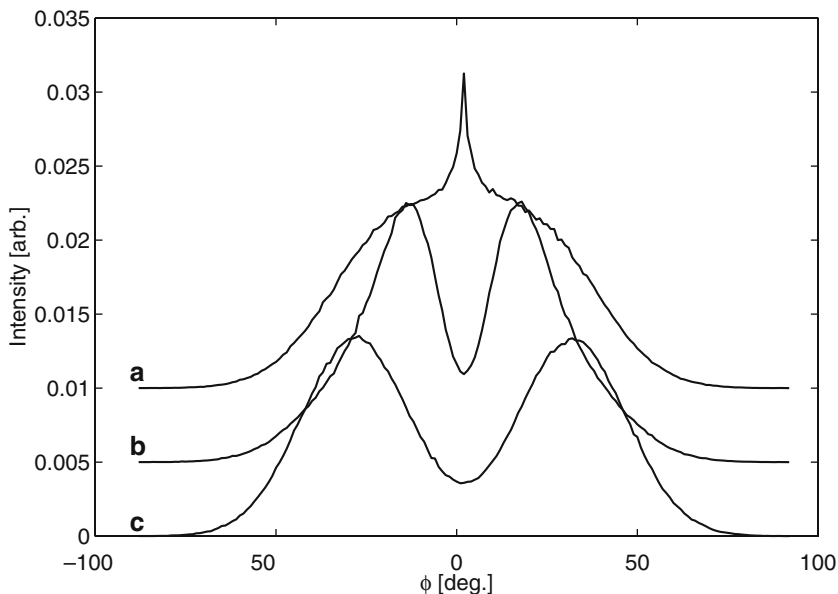
Fig. 8 The effect of the cross-sectional shape of the cells on the intensity curve of reflection (200) when the STG is used. Curve A presents cells with round, B hexagonal and C rectangular cross sections. Computations were made for normally distributed MFA with a mean value of 30° and STD of 15°

The obtained MFA increases as ρ increases (Table 1). However, for Norway spruce the effect may be smaller than the accuracy of determination. If the samples are cut from one annual ring in tangential direction, which is common for STG experiment, the effect of spiral grain can be neglected (Table 1). For large values of ρ the determined MFA becomes clearly too large. According to Table 1 large deviations in spiral grain or tips (large STDs of ρ) tend to increase the MFA obtained using PTG and the variance method and decrease the MFA obtained using PTG and the fitting method. When using STG and peak fitting the mean MFA tends to increase. This is attributed to the fitting; if the STD of MFA is large it is difficult to separate contributions from different cell walls.

Radial walls of Norway spruce contain a considerable amount of bordered pits, which can also affect the determined MFA values. In Sarén et al. (2004) the mean MFA values were determined experimentally from both radial and tangential walls of the same wood material using PTG and the fitting method taking the shape of the cell into account appropriately. The mean MFA determined from radial walls was roughly 2° larger than those determined from tangential walls.

Conclusions

In this paper a general form for diffraction conditions was derived and the effects of the shape of the cell and the spiral grain on the MFA determinations for Norway spruce using PTG and STG were discussed. The conditions are valid also for other wood material with small MFA and other crystalline materials with similar symmetry as wood cells. Monte Carlo method was used to calculate the intensity profiles. This method is not convenient for data analysis, but can be used for verification of the validity of data-analysis methods.

According to the calculations the use of STG is favourable, since the data analysis is simple and reliable. The most straightforward way for determining the mean MFA is the use of the 004 reflection since this reflection is affected neither by the shape of the cell nor the orientation of the cells in the sample. However, the intensity arising from other reflections contaminates the solved MFA distribution at larger angles.

Results indicate that small variations in the cell orientation do not affect the mean MFA considerably for Norway spruce. When using STG and the reflection 200 the cross-sectional shape of the cells should be taken into account by using a suitable fitting model. In practice, small deviations from rectangular cell cross sections may not affect the fitted mean MFA considerably. The fitting of the extra peak at $\phi = 0°$ may complicate the analysis of data obtained using PTG but it is well justified according to calculations presented in this paper. For cells with round cross sections the model presented by Perret and Ruland (1969) can be used.

The variance method (Evans 1999) requires some experimental coefficients, which may be species specific. Nevertheless, it may suit well for screening a large set of samples. By using the peak-fitting method one can determine the shape of the MFA distribution in addition to the mean MFA. It is, however, more laborious than the variance method.

References

Abe H, Ohtani J, Fukuzawa K (1991) FE-SEM observations on the microfibrillar orientation in the secondary wall of tracheids. IAWA B 12:431–438

Anagnost SE, Mark RE, Hanna RB (2000) Utilization of soft-rot cavity orientation for the determination of microfibril angle, Wood. Fib Sci 32:81–87

Andersson S, Serimaa R, Torkkeli M, Paakkari T, Saranpää P, Pesonen E (2000) Microfibril angle of Norway spruce [*Picea abies* (L.) Karst.] compression wood: comparison of measuring techniques. J Wood Sci 46:343–349

Andersson S, Serimaa R, Paakkari T, Saranpää P, Pesonen E (2003) Crystallinity of wood and the size of cellulose crystallites in Norway spruce (*Picea abies*). J Wood Sci 49:531–537

Bailey IW, Vestal MG (1937) The significance of certain wood-destroying fungi in the study of the enzymatic hydrolysis of cellulose. J Arnold Arbo 18:196–205

Batchelor WJ, Conn AB, Parker IH (1997) Measuring the microfibril angle of fibers using confocal microscopy. Appita J 50:377–380

Booker RE, Sell J (1998) The nanostructure of the cell wall of softwoods and its functions in a living tree. Holz als Roh und Werkstoff 58:1–8

Cave ID (1966) Theory of X-ray measurement of microfibril angle in wood. Forest Prod J 16:37–42

Cave ID, Walker JCF (1994) Stiffness of wood in fast-grown plantation softwoods: the influence of microfibril angle. Forest Prod J 44:43–48

Cave ID (1997a) Theory of X-ray measurement of microfibril angle in wood, part 1. Wood Sci Tech 31:143–152

Cave ID (1997b) Theory of X-ray measurement of microfibril angle in wood, part 2. Wood Sci Tech 32:225–234

Donaldson LA (1991) The use of pith apertures as windows to measure microfibril angle in chemical pulp fibers. Wood Fib Sci 23:290–295

Evans R (1999) A variance approach to the X-ray diffractometric estimation of microfibril angle in wood. Appita J 52:283–289

Guinier A (1994) X-ray diffraction in crystals, imperfect crystals and amorphous bodies. Dover, USA

Harris JM (1988) Spiral grain and wave phenomena in wood formation. Springer, Berlin Heidelberg New York

Harris JM, Meylan BA (1965) The influence of microfibril angle on longitudinal and tangential shrinkage in Pinus radiata. Holzforschung 19:144–153

Klug HP, Alexander LE (1974) X-ray diffraction procedures for paracrystalline and amorphous materials, 2nd edn. Wiley, New York

Kozlowski TT, Winget CH (1963) Patterns of wood movement in forest trees. Bot Gaz 124:301–311

Lichtenegger H, Müller M, Paris O, Rieker Ch, Fratzl P (1999) Imaging of the helical arrangement of cellulose fibrils in wood by synchrotron X-ray microdiffraction. J Appl Cryst 32:1127–1133

Lichtenegger H, Reiterer A, Stanzl-Tschegg S, Fratzl P (2001) Comment about "The measurement of the micro-fibril angle in soft-wood" by K.M. Entwistle and N. J. Terrill. J Mater Sci 20:2245–2247

Lotfy M, El-osta M, Kellogg RM, Foschi RO, Butters RG (1973) A Direct X-ray Technique for Measuring Microfibril Angle. Wood Fiber 5:118–127

Nishiyama Y, Langan P, Chanzy H (2002) Crystal structure and hydrogen-bonding system in cellulose Iβ from synchrotron X-ray and neutron fiber diffraction, J. Am Chem Soc 124:9074–9082

Paakkari T, Serimaa R (1984) A study of the structure of wood cells by X-ray diffraction. Wood Sci Tech 31:79–85

Paris O, Müller M (2003) Scanning X-ray microdiffraction of comples materials: Diffraction geometry considerations. Nuc Inst Met Phys Res B 200:390–396

Peura M, Müller M, Serimaa R, Vainio U, Sarén MP, Saranpää P, Burghammer M (2005) Structural studies of single wood cell walls by synchrotron X-ray microdiffraction and polarised light microscopy. Nucl Inst Meth B 238:16–20

Perret R, Ruland W (1969) Single and multiple X-ray small-angle scattering of carbon fibres. J Appl Crystallogr 2:209–218

Prud'homme R, Noah J (1975) Determination of fibril angle distribution in wood fibers: A comparison between X-ray diffraction and the polarized microscope method. Wood and fiber 6:282–289

Sarén MP, Andersson S, Serimaa R, Paakkari T, Saranpää P, Pesonen E (2001) Structural 506 Variation of Tracheids in Norway Spruce (Picea abies [L.] Karst.). J Stuct Biol 136:101–109

Sarén MP, Serimaa R, Andersson S, Saranpää P, Keckes J, Fratzl P (2004) Effect of growth rate on mean microfibril angle and cross-sectional shape of the tracheids in Norway sprice. Trees 18:345–362

Sarén MP, Peura M, Serimaa R (2005a) Interpretation of microfibril angle distributions in wood using microdiffraction experiments on single cells. J X-Ray Sci Tech 13:1–7

Sarén MP, Serimaa R, Tolonen Y (2005b) Determination of fiber orientation in Norway spruce using X-ray diffraction and laser scattering. Holz als Roh und Werkstoff (in press)

Verbelen JP, Stickens D (1995) In-vivo determination of fibril orientation in plant-cell walls with polarization CSLM. J Microsc Oxford 177:1–6

Wobst J, Olivervillanueva JV, Doebel R (1994) Variability of fiber angle in wood of ash (Fraxinus-Excelsior L.) and Douglas fir (Pseudotsuga-mensii (mirb) Franco). Holz als rohr- und Werkstoff. 52:342–346

Yamamoto H, Okuyama T, Yoshida M (1993) Method of determining the man microfibril angle of wood over a wide range by the improved Cave's method. Mokuzai Gakkaishi 39:375–381

Ye C, Sundström MO, Remes K (1994) Microscopic transmission ellipsometry—measuring of the fibril angle and the relative phase retardation of single, intact wood pulp fibers. Appl Optics 33:6626–6637